Complexation of arsenite, arsenate, and monothioarsenate with oxygen-containing functional groups of natural organic matter: An XAS study

Biswas, A.; Besold, J.; Sjöstedt, C.; Gustafsson, J. P.; Scheinost, A. C.; Planer-Friedrich, B.;

Complexation of arsenite, arsenate, and monothioarsenate to alcoholic functional groups of natural organic matter: Insights from X-ray absorption spectroscopy

Ashis Biswas[1,2]*, Johannes Besold[1], Carin Sjöstedt[3], Jon Petter Gustafsson[3], Andreas C. Scheinost[4,5], Britta Planer-Friedrich[1]

[1]*Department of Environmental Geochemistry, Bayreuth Center for Ecology and Environmental Research (BAYCEER), Bayreuth University, 95440 Bayreuth, Germany*

[2]*Department of Earth and Environmental Sciences, Indian Institute of Science Education and Research (IISER) Bhopal, Bhopal Bypass Road, Bhauri 462066, Madhya Pradesh, India*

[3]*Department of Soil and Environment, Swedish University of Agricultural Sciences, Box 7014, 750 07, Uppsala, Sweden*

[4]*The Rossendorf Beamline (ROBL) at ESRF, 38043 Grenoble, France*

[5]*Institute of Resource Ecology, Helmholtz-Zentrum Dresden-Rossendorf (HZDR), Bautzner Landstraße 400, 01328 Dresden, Germany*

*Contact and corresponding author: Ashis Biswas (phone: +91 755 269 1389; e-mail: ashis@iiserb.ac.in**)**

17   **TOC Art**

18

19

ABSTRACT

This study investigated the potentiality of arsenite (~~As(III)~~), arsenate (~~As(V)~~), and monothioarsenate (MTAs(V)) complexation to alcoholic groups of natural organic matter (NOM). The extent of complexation was highest for As(III), followed by MTAs(V) and As(V). Complexation was higher at pH 7.0 than at pH 4.5 for As(III) and As(V), vice versa for MTAs(V) due to partial transformation to As(III) at pH 4.5. Conditional distribution coefficients were considerably lower than those for complexation through organic thiol groups, but comparable to those for ternary complexation through Fe^{3+} bridging. EXAFS modelling of the As K-edge spectra revealed monodentate and bidentate complexation of the AsO_3 pyramid but tridentate complexation of the AsO_4 and the $AsSO_3$ tetrahedra to alcoholic groups of peat. The higher denticity and an observed longer As-C interatomic distance in As(V)- and MTAs(V)- treated peat - as compared to As(III)-treated peat - is attributed to electrostatic repulsion between negatively charged peat and As species. This study implies that complexation through alcoholic groups of NOM can be an additional or alternative mode of As sorption and depending on acidity of the functional NOM groups, As(V) species can have a higher mobility than arsenite in NOM-rich environments.

2

INTRODUCTION

Over the last four decades, the natural and anthropogenic occurrences of elevated concentrations of arsenic (As) in surface waters, groundwaters, and agricultural soils have been highlighted as a potential environmental concern in many parts of the world.[1–3] It is estimated that only in Southeast Asia more than 100 million of people are at risk of chronic As toxicity from drinking water and food consumption.[4] Therefore, it is necessary to characterize different biogeochemical processes that regulate the mobility of As in the aquatic and terrestrial ecosystems.

Formation and inter-conversion of different As species determine the extent of its mobility in the environment.[1] Two most commonly reported inorganic As species are penta-valent arsenate (As(V)) and tri-valent arsenite (As(III)) which predominate under strongly oxidizing conditions and moderately oxidizing to moderately reducing conditions, respectively.[1] After recent advances in analytical speciation technique, it has become evident that under anoxic sulfidic conditions thiolated penta-valent As species, so-called thioarsenates ($H_xAsS_nO_{4-n}^{3-x}$; n = 1−4; x = 1−3), can also be formed in significant quantities under diverse natural settings.[5–11] Extent of sorption of these As species onto different mineral matters, specially metal oxyhydroxides in soils and sediments is identified as one of the key regulating processes for their mobility in the environment.[1,12–14] Recently, a series of studies have highlighted the potentiality of natural organic matter (NOM) as an alternative or additional sorbent for As and its regulatory role in the As mobilization and transport process in the surface and sub-surface environments.[15–21]

Natural organic matter, being the decomposition product of animal, plant and soil biomass is abundant in aquatic and terrestrial ecosystems.[16] It has a complex structure with a variety of functional groups, such as carboxylic, alcoholic, esteric, quinone, amino, nitroso, thiol, hydroxyl etc., which are mostly negatively charged at near-neutral pH.[16] Several mechanisms for the binding of As(V) and As(III) to NOM have been put forward. One spectroscopically well characterized mechanism is the formation of ternary complexes through polyvalent metal cation (e.g. Fe^{3+}, Al^{3+}, Ca^{2+}, etc.) bridging between negatively charged or neutral As species and negatively charged NOM (As-M-NOM; M represents polyvalent metal cations).[17,22–26] Another mechanism is the binary complexation by direct binding of As species to the specific functional group of NOM. The most prominent site for such binary complexation can be organic thiol groups (–SH).[21,27] Langner et al.[21] by using X-ray absorption spectroscopy (XAS) have found

69   almost 100% of As(III) to be bound to thiol groups in the deep peat layer of a minerotrophic peat

70   bog (*Gola di Lago*). A follow-up study has shown that As(III) binding by thiol group can be

71   competitive to its binding by ferrihydrite.[28] Recently, Catrouillet et al.[29,30] have developed a

72   geochemical model for As(III) complexation to NOM by thiol group and via Fe^{2+} and Fe^{3+}

73   bridging. Liu and Cai,[31] on the other hand, have reported two types of binding sites (strong and

74   weak sites) to be involved during binary complexation of As(III) with Aldrich Humic Acid

75   (AHA); although, they did not attempt to characterize the binding sites.

76   Few studies have highlighted that alcoholic (–OH) groups (aliphatic and/or aromatic, specially

77   phenol), a highly abundant functional group in NOM,[32] can also be a potential binding site for

78   binary complexation of As species to NOM. For example, Buschmann et al.[18] in a dialysis

79   experiment found that 26% As(III) and 62% As(V) of total spiked concentrations bound to AHA

80   and estimated that under environmentally relevant conditions at least 10% As(V) should be

81   bound to dissolved organic carbon (DOC) in aquatic environments. They hypothesized that OH^-

82   ligand exchange reaction between As species and alcoholic groups of NOM could be the

83   underlying mechanism of such bindings; although, they did not present any spectroscopic

84   evidence in support of their hypothesis. Lenoble et al.[33] have investigated the interaction of

85   As(III) and As(V) to Suwanee River Humic Acid (SRHA) in the absence and presence of Ca^{2+}

86   by fluorescence spectroscopy. Based on sorption data and fluorescence quenching phenomena of

87   SRHA they concluded the formation of only a binary complex for As(III) and a mixture of

88   binary and Ca^{2+} bridged ternary complexes for As(V). They have determined the stability

89   constant of these complexes assuming monodentate binding to alcoholic group of SRHA,

90   without further effort to characterize the type of functional group involved in the complexation

91   and mode of binding. Evidence of As-O-C bond formation by ligand exchange reaction between

92   alcoholic group of NOM and As species is given by Hoffmann et al.[26] and Guénet et al.[34] During

93   modelling of As K edge EXAFS spectra of the samples obtained by equilibrating As(III) with Fe

94   spiked peat Hoffmann et al.[26] had to include C in addition to Fe for the second shell. They have

95   determined coordination numbers (CN) of 1.5 to 2.0 for C at the distance of 2.70 to 2.77 Å from

96   the As. However, they have mentioned that due to signal contribution from Fe backscatterer at

97   similar distance, the CN of C must be treated with caution. They have further estimated that at

98   least 27% of total As(III) was bound to phenolic groups, in addition to ternary complexation via

99   Fe^{3+} bridging. Similarly, Guénet et al.[34] have provided XAS based evidence for the complexation

4

100 of As(V) and As(III) mixtures to alcoholic groups of organic matter, in addition to their bindings
101 to Fe nanoparticle aggregates in the size fraction of 5-0.2 µm during oxidation of reduced soil
102 suspension solution. However, to the best of our knowledge, so far it has never been attempted to
103 investigate the extent of As(III) and As(V) bindings to NOM by complexation exclusively to the
104 alcoholic group, with spectroscopic evidence of As-O-C bond formation. Unavailability of this
105 information obscures the potentiality of As(III) and As(V) bindings to NOM when polyvalent
106 metal cation content in the system is too low for ternary complexation and thiol group content in
107 NOM is not large enough to make significant thiol coordination. It is worth highlighting that the
108 complexation of thioarsenate to alcoholic group of NOM has never been tested at all.

109 The objective of the present study was to investigate the potentiality and determine the structural
110 parameters for ligand exchange binary complexation of different As species (including
111 thioarsenate) to alcoholic groups of NOM. The objective was accomplished by equilibrating
112 individual As species with low metal containing purified-peat (as a representative for NOM)
113 under anoxic conditions, followed by determining the local coordination environment (up to 4 Å)
114 of As in the peat by As K edge XAS analysis. The findings of this study will help to better
115 constrain the geochemical model for simulating the interaction of As species with NOM in
116 aquatic and terrestrial environments. In general, this study will also develop our limited
117 understanding of neutral to oxyanionic species complexation to NOM, a topic that is not as
118 developed as metal cation complexation to NOM.[18]

119 **MATERIALS AND METHODS**

120 **Materials.** This study used low metal containing purified-peat as a model NOM compound.
121 Collection, purification, and characterization of this peat are presented in Besold et al.[35]
122 Monothioarsenate (hereafter referred as MTAs(V)) was used as the representative of thioarsenate
123 species, since it is often reported as the major thioarsenic species formed under diverse natural
124 settings and is structurally analogous to the As(V).[6,35–37] Because there is no commercial
125 standard, MTAs(V) was synthesized in the laboratory, with a purity of 90% (5% arsenate and 5%
126 arsenite).[35] All other chemicals of analytical grade, including As(III) and As(V) standards, were
127 purchased from Fluka, Alfa Aesar, or Sigma-Aldrich. All the glasswares used in this study were
128 acid-washed and dried before use.

Sorption experiment. An equilibrium-sorption experiment was conducted for individual As species at pH 4.5 ($\pm$0.3) and 7.0 ($\pm$0.3). For this experiment, 0.2 g of dry peat was incubated with variable concentrations (0 – 1000 µM) (0 – 4.6 mmol As/mol C) of each As species in an anoxic background electrolytic solution of 30 mM NaCl in glass septum bottles capped and sealed with butyl rubber stoppers and aluminum caps. Incubation was conducted for 96 h in an end over end shaker in the dark under anoxic conditions (pO_2 <1 ppm) at ambient temperature. The duration of 96 h was selected for incubation so that the results can be directly compared to the studies of Hoffmann et al.[26,27] which have used the same peat to investigate As(III) bindings through binary organic thiol coordination and Fe^{3+} bridged ternary complex formation. To avoid microbial activity, 0.15 mM NaN_3 (0.75 mmol/mol C) was added to the reaction medium. The desired pH was adjusted with anoxic HCl and NaOH solution. After equilibration, the peat-solution slurry was filtered through 0.2 µm nylon filter using a vacuum filtration unit inside the glove box. The peat residue was freeze-dried, homogenized, and stored in the dark at ambient temperature inside the glove box until analyses. The amount of As sorbed to peat was determined after microwave-assisted digestion followed by quantification of As by inductively coupled plasma-mass spectrometry (ICP-MS).[35] The conditional distribution coefficient (K_{OC}) (L/kg) of As was determined as: $K_{OC} = C_P/C_S$, where C_P and C_S represent As concentration in peat (µg/kg) and As concentration in solution (µg/L) after equilibration, respectively. C_S was determined by subtracting the amount of As sequestered into peat from the solution.

Arsenic K edge XAS analysis. To determine the local coordination environment of As in the peat after equilibration, As K edge (11867 eV) XAS analysis was performed at the Rossendorf Beamline (ROBL) at the European Synchrotron Radiation Facility (ESRF), Grenoble, France and at the beamline 11-2 of the Stanford Synchrotron Radiation Lightsource (SSRL), Stanford, USA. To aid the modelling of the sample spectra, triethoxyarsine (($C_2H_5O)_3As$) (TEA) was measured as a reference standard at ROBL, ESRF. Samples were measured in fluorescence mode, while the TEA standard was measured in transmission mode. Samples and the standard were measured at about 15 K using a He cryostat to avoid beam damage and to minimize thermal disorder in the structure. Details on beamline setup, sample preparation, analysis, data reduction, and modelling are provided in the supporting information.

RESULTS AND DISCUSSION

Complexation of As species to peat. Amounts of As sorbed to peat at different equilibrated concentrations of the three As species at pH 4.5 and 7.0 are illustrated in Figure 1. Among the three tested species, maximum sorption was observed for As(III), followed by MTAs(V) and As(V). Earlier studies have reported higher sorption of As(V) to AHA and SRHA compared to As(III);[18,22,38] the possible reason for this inconsistency is discussed in the following section after determination of the binding mechanism. The maximum sorption capacity of the peat was not exhausted even with the highest equilibrated As(III) concentration of 1000 µM (4.6 mmol As/mol C). In agreement with earlier studies,[18,22,31,33,38] the sorption of As(III) and As(V) was higher at pH 7.0. The pH effect was more prominent for As(III) compared to As(V). However, for MTAs(V) the sorption was higher at pH 4.5, which can be attributed to the partial transformation of MTAs(V) to As(III) at this pH, as reflected by the XANES spectra discussed in the following section. The calculated log K_{OC} (L/kg) at pH 7.0 were 0.83 – 1.01 (mean: 0.90) for As(III), 0.40 – 0.56 (mean: 0.47) for MTAs(V), and 0.34 – 0.41 (mean: 0.38) for As(V); at pH 4.5 corresponding values were 0.73 – 0.85 (mean: 0.78), 0.44 – 0.66 (mean: 0.52), and 0.31 – 0.38 (mean: 0.35). With experimental uncertainty, the log K_{OC} decreased with the increase of equilibrated As concentration (more specifically with the increase of equilibrated As/NOM ratio as the amount of NOM was fixed to 0.2 g) in the system for all three As species at both pH (Figure SI-1). Although no explanation is offered, earlier studies have also reported similar decreasing trend of distribution coefficients for As(V) and As(III) binding to NOM with increasing As/NOM ratios.[18,31] Hoffmann et al.[26,27] have determined the log K_{OC} values at pH 7.0 by equilibrating 0.275 mmol As(III)/mol C of the same peat spiked with variable amount of S(-II) and Fe^{3+}. The values for As(III) at pH 7.0 of the present study (0.83 – 1.01) are considerably lower than the values (0 – 2.9) obtained after spiking with S(-II), but comparable to that (1.2 – 1.5) obtained after spiking with Fe^{3+}.

EXAFS modelling and complexation mechanism. Normalized As K edge XANES spectra of peat after equilibration with As(III), As(V), and MTAs(V) at two pH together with various reference standards are displayed in Figure SI-2. The E_0 of peat equilibrated with As(III) and As(V) at both pH appeared at the respective position of As(III) (~11869 eV) and As(V) (~11873 eV) reference standards, indicating no species transformation during equilibration. Similarly, MTAs(V) was not transformed to other species at pH 7.0, indicated by the similar E_0

7

189 of the samples and reference standard at ~11871 eV. However, at pH 4.5 the spectra of the two

190 MTAs(V) treated peat samples showed two humps at the position of MTAs(V) and As(III)

191 standards, suggesting partial transformation of MTAs(V) to As(III) during equilibration at this

192 pH. Our earlier study [35] has shown that MTAs(V) can be transformed into As(III) at acidic pH in

193 the presence of S(-II) treated peat, which makes the transformation reaction kinetically feasible

194 by sorbing As(III) (product of transformation) from the solution. The present study suggests that

195 this acid-assisted transformation will be feasible in the presence of any sorbent that sorbs As(III)

196 more strongly than MTAs(V). Based on the findings from XANES spectra, EXAFS modelling

197 was performed for all analyzed peat samples equilibrated with As(III) and As(V) at two pH and

198 MTAs(V) at pH 7.0 only; for the two peat samples equilibrated with MTAs(V) at pH 4.5, linear

199 combination fit (LCF) analysis was performed.

200 To better constrain sample spectra during EXAFS modelling, the spectrum of TEA was modelled

201 first (Figure SI-3). The major peak at R+ΔR ~1.3 Å in the FT is due to the nearest neighbor O of

202 the AsO_3 pyramid. This major peak was followed by a small FT peak at R+ΔR ~2.2 Å, which

203 can be assigned to C in the second shell.[26,39] Quantitative structural parameters of these two

204 shells were determined by shell-fit analysis. The final model for TEA included As-O and As-C

205 single-scattering (SS) paths and triangular As-O-C multiple-scattering (MS) path.

206 Parameterization (CN: path degeneracy or coordination number, R: interatomic distance or mean

207 half path length (bond length for first shell atom), and σ^2: Debye – Waller parameter) of these

208 paths are presented in Table SI-1. Furthermore, the triangular As-O-O MS path within the AsO_3

209 pyramid (Table SI-1) was also tested, but finally discarded, since it did not improve the fit

210 significantly. The fitted R and σ^2 of the As-O and As-C paths were 1.78 Å and 0.0021 and 2.78

211 Å and 0.0059, respectively (Table SI-2), which are consistent with reported values.[26]

212 The k^3-weighted As K edge EXAFS spectra and their corresponding FT (magnitudes and real

213 parts) of the peat samples equilibrated with As(III) and As(V) at the two pH and MTAs(V) at pH

214 7.0 are shown in Figure 2. Qualitative Morlet wavelet transforms (WT) analysis of As K edge

215 EXAFS spectra of the samples did not indicate the presence of any heavy backscatterer in the

216 second or higher shell (Figure SI-4). Similar to TEA, FT of the k^3-weighted EXAFS spectra of

217 As(III)-, As(V)-, and MTAs(V)-treated peat samples were characterized by two peaks: a major

218 peak at R+ΔR ~1.3 Å corresponding to nearest neighbor O in the first shell and a small peak at

219   R+ΔR ~2.2 Å for As(III) (Figure 2A) and ~2.3 Å for As(V) and MTAs(V) (Figure 2B,C)

220   corresponding to C in the second shell. For MTAs(V)-treated peat samples, an additional peak

221   appeared at R+ΔR ~1.8 Å (Figure 2C), which can be attributed to S in the first shell.[36]

222   Accordingly, for all peat samples except #As(V)/4.5/500, inclusion of As-O and As-C SS paths

223   (Table SI-1) in the structural model was essential to fit the sample spectra. For the three

224   MTAs(V)-treated samples, additional As-S SS path (Table SI-1) was also necessary for the

225   fitting. For the sample #As(V)/4.5/500, despite the small FT peak at R+ΔR ~2.3 Å the addition

226   of As-C SS path to the model after As-O SS path and MS paths within the AsO_4 tetrahedra

227   (discussed latter) did not improve the fit significantly according to the F-Test, although it

228   decreased the R-factor. Although, the As-O-C MS path was essential to fit the TEA spectrum,

229   this MS path (constrained similarly as for TEA, Table SI-1) did not improve the fit significantly

230   for any samples according to the set criteria for the MS path. For the As(III)-treated peat samples

231   the triangular As-O-O MS path within the AsO_3 pyramid (Table SI-1) was tested and found to be

232   significant only for the sample #As(III)/7.0/150 by decreasing the redχ^2 by 31% compared to the

233   model with only As-O SS path. However, for all As(V) treated samples, when three MS paths

234   within the AsO_4 tetrahedra, namely, triangular As-O-O, colinear As-O-As-O, and non-colinear

235   As-O-As-O (Table SI-1) were included together in the fit, decreased the redχ^2 on average by

236   52% (38-69%). Similarly, addition of triangular As-O-O and colinear As-O-As-O MS paths

237   within the $AsSO_3$ tetrahedra (Table SI-1) decreased the redχ^2 in the MTAs(V)-treated samples on

238   average by 30% (23-36%), compared to the model with only As-O and As-S SS paths.

239   Therefore, the final fit model included As-O and As-C SS paths for As(III)-treated samples

240   (additional triangular As-O-O MS path for #As(III)/7.0/150); As-O and As-C (except

241   #As(V)/4.5/500) SS paths and three MS paths within the AsO_4 tetrahedra for As(V)-treated

242   samples, and As-O, As-S, and As-C SS paths and two MS paths within the $AsSO_3$ tetrahedra for

243   MTAs(V)-treated samples. The final fits are displayed in Figure 2 and EXAFS parameters are

244   listed in Table 1.

245   In the As(III)-treated peat samples the average R_{As-O} was 1.79 ± 0.01 Å (±std. dev.) (range: 1.78

246   – 1.80 Å), consistent with the reported As-O bond lengths in the AsO_3 pyramid.[39,40] For As-C

247   path, the fitted R_{As-C} was 2.73 ± 0.01 Å (2.73 – 2.74 Å) with CN of 1.7 ± 0.6 (1.0 – 2.4). Despite

248   similar oxidation state of As, the fitted R_{As-C} was relatively longer in TEA (2.78 Å) compared to

249   that in peat, which can be attributed to the liquid state of the TEA standard. The fitted R_{As-C}

250 values suggest that the AsO_3 pyramids were complexed to peat probably through alcoholic

251 groups (aliphatic and/or aromatic) instead of carboxylic group because, in case of complexation

252 through carboxylic groups, shorter R_{As-C} values (2.58 – 2.68 Å) are expected due to possible

253 hydrogen bonding between the H atom of the As(III) and the carbonyl O of the carboxyl

254 group.[26,39] The fitted R_{As-C} and CN_{As-C} values in peat are consistent with the values (R: 2.70 –

255 2.77 Å, CN: 1.5 – 2.0) determined by Hoffmann et al.[26] for the Fe-spiked peat equilibrated with

256 As(III) (0.275 mmol As(III)/mol C) at the pH of 7.0, 8.4, and 8.8. They have determined

257 relatively longer R_{As-C} at pH ≥8.4 compared to that at pH 7.0; no such difference was observed in

258 the studied pH range (4.5 to 7.0) of the present study. To determine the exact mode of binding, in

259 the next step we fixed the CN_{As-C} to either 1.0 (Figure SI-5) or 2.0 (Figure SI-6) in the fit model,

260 while keeping the fit strategy for the rest of the parameters unchanged. Results show that for the

261 sample #As(III)/7.0/150 redχ^2 was decreased further when CN_{As-C} was fixed to 1.0 (Table SI-3

262 vs. Table 1), while for the sample #As(III)/7.0/1000, #As(III)/4.5/1000, and #As(III)/4.5/500,

263 redχ^2 was decreased when CN_{As-C} was fixed to 2.0 (Table SI-4 vs. Table 1). For the sample

264 As(III)/7.0/100, redχ^2 was increased in both cases; however, the increment was more when CN_{As-C}

265 was fixed to 2.0 (Tables-SI-3 and 4 vs. Table 1). Therefore, we conclude that irrespective of

266 pH when equilibrated As(III) concentration is low (≤150 µM; 0.69 mmol As(III)/mol C) each

267 AsO_3 pyramid gets complexed to one alcoholic group of peat (monodentate, Figure 3A);

268 whereas, when equilibrated As(III) concentrations is high (≥500 µM; 2.3 mmol As(III)/mol C)

269 the preferential binding mode is the complexation of each AsO_3 pyramid to two alcoholic groups
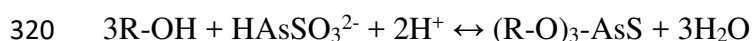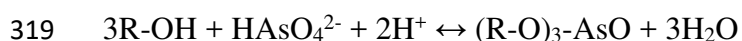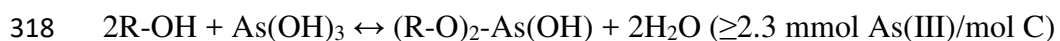
270 (bidentate, Figure 3B).

271 Because of higher oxidation state of As, in the As(V)-treated peat the R_{As-O} was considerably

272 shorter (1.69 ± 0.01 Å, 1.68 – 1.69 Å) compared to the R_{As-O} in the As(III)-treated peat samples.

273 These fitted R_{As-O} values are similar to the reported As-O bond lengths within the AsO_4

274 tetrahedra.[41] The fitted R_{As-C} and CN_{As-C} were 2.83 ± 0.01 Å (2.82 – 2.84 Å) and 3.2 ± 0.2 (3.0 –

275 3.4), respectively, comparatively higher than that in the As(III)-treated peat samples. When

276 CN_{As-C} was set to 3.0 in the model (Figure SI-7), redχ^2 was decreased on average by 6% for all

277 the samples (Table SI-5 vs. Table 1), suggesting that each AsO_4 tetrahedra was attached to three

278 alcoholic groups of the peat (Figure 3C). It is worth mentioning that even in the sample

279 #As(V)/4.5/500, although fit improvement because of inclusion of the As-C path in the model

280 was not statistically significant, the fitted R_{As-C} (2.79 Å) and CN_{As-C} (2.3) were comparable to

281   other samples and redχ^2 was decreased by 5% when CN_{As-C} was set to 3.0 (Table SI-6). Guénet et

282   al.[34] have determined comparable R_{As-C} (2.85-2.86 Å), but relatively smaller CN_{As-C} (1.7 – 2.1)

283   for the mixture of As(V) and As(III) in the 5 – 0.2 µm size fraction during oxidation of the

284   reduced soil suspension. The smaller CN_{As-C} may be result from the presence of As(III) in the

285   system; however, in that case a shorter R_{As-C} is also expected. A more probable alternative

286   explanation is that this can be due to the low As-organic carbon ratio (~0.04 mmol As/mol C) in

287   the solution at the starting of oxidation of the reduced soil suspension. This reason will implicate

288   that similar to As(III), at the low concentration of As(V), each AsO_4 tetrahedra will probably be

289   attached to a lower number (<3.0) of alcoholic groups. Similar to As(III) treatment, there was no

290   effect of change in the equilibrium pH on the fitted EXAFS parameters for the As(V) treatment

291   (Table 1).

292   In the MTAs(V)-treated peat, the fitted R_{As-O} was 1.72 ± 0.01 Å (1.71 – 1.72 Å), relatively

293   longer than R_{As-O} in As(V)-treated peat but shorter than As(III)-treated peat. The R_{As-S} was

294   determined as 2.10 ± 0.02 Å (2.08 – 2.11 Å), indicating S was double bonded to As.[36] Suess et

295   al.[36] have determined R_{As-O} and R_{As-S} in pure MTAs(V) standard by EXAFS modelling as 1.70 Å

296   and 2.13 Å, respectively. Despite same oxidation state of As, relatively longer R_{As-O} in the

297     $AsSO_3$ tetrahedra compared to that in the AsO_4 tetrahedra in peat can be attributed to the less

298   positive partial charge on the central As atom because of replacement of the double bonded O

299   with double bonded S, which is less electronegative. For As-C path, the fitted R and CN were

300   2.80 ± 0.02 Å (2.78 – 2.82 Å) and 3.0 ± 0.4 (2.6 – 3.4), respectively, similar to the values

301   obtained for As(V)-treated peat. Again, fixing of CN_{As-C} to 3.0 (Figure SI-8) decreased the redχ^2

302   on average by 6% for all the samples (Table SI-7 vs Table 1), suggesting each $AsSO_3$ tetrahedra

303   was attached to three alcoholic groups of the peat (Figure 3D). To the best of our knowledge this

304   is the first study that determines the local coordination environment of As when MTAs(V) is

305   complexed to NOM. Since the number of alcoholic group in the peat equilibrated with all three

306   As species was the same, the higher CN_{As-C} in the As(V)- and MTAs(V)-treated peat (CN 3)

307   explains why the extent of sorption of these two As species was less compared to As(III) (CN 1-

308   2) (Figure 1). Furthermore, increase of CN_{As-C} with the increase of equilibrated As concentration

309   (clearly identified for As(III) system) was probably the reason for decreased log K_{OC} with the

310   increase of As/NOM ratio (Figure SI-1). The LCF analysis of the two peat samples equilibrated

311   with MTAs(V) at the pH 4.5 (Figure SI-9) indicated they were a mixture of almost equal

11

312   proportion (Table SI-8) of MTAs(V) (44 – 58%) and As(III) (44 – 60%) complexed to peat with

313   the above determined coordination environments.

314   Above presented modelling of the As K edge EXAFS data of peat equilibrated with different As

315   species has identified two types of complex to be formed for As(III) and one each for As(V) and

316   MTAs(V) (Figure 3), with the following reaction stoichiometry:

317   R-OH + As(OH)$_3$ ↔ R-O-As(OH)$_2$ + H$_2$O (≤0.69 mmol As(III)/mol C)

318   2R-OH + As(OH)$_3$ ↔ (R-O)$_2$-As(OH) + 2H$_2$O (≥2.3 mmol As(III)/mol C)

319   3R-OH + HAsO$_4$$^{2-}$ + 2H$^+$ ↔ (R-O)$_3$-AsO + 3H$_2$O

320   3R-OH + HAsSO$_3$$^{2-}$ + 2H$^+$ ↔ (R-O)$_3$-AsS + 3H$_2$O

321   The formation of ester of As(III) and As(V) acid with alcohol is well known.[42–44] The underlying

322   mechanism for this esterification is the nucleophilic attack by the alcoholic group to the partially

323   positively charged As atom in the As species.[18] An increase of nucleophilicity of the alcoholic

324   group and a partial positive charge on the As atom increases the rate and thereby extent of

325   complex formation. Since the nucleophilicity of the alcoholic group increases with an increase of

326   pH, it is expected that the extent of complex formation between As species and the alcoholic

327   group will be more at higher pH, which explains the higher sorption of As(III) and As(V) at pH

328   7.0 compared to 4.5 in the present study (Figure 1). Few earlier studies have reported that

329   complexation of As(III) and As(V) to NOM is optimum around near-neutral pH,[18,22] because at

330   high pH alcoholic group experiences competition with hydroxyl ion from the reaction medium

331   for the nucleophilic attack to the As center. Among the three tested As species, partial positive

332   charge on the central As atom is highest in the As(V), followed by MTAs(V) and As(III);

333   because in As(V) there is an additional O, double bonded to As compared to As(III) and in

334   MTAs(V) this double bonded O is replaced by the less electronegative S. Therefore, considering

335   the partial positive charge on an As atom the expected order of the extent of complexation for the

336   three As species would be As(V) >MTAs(V) >As(III). In agreement with this expected order

337   earlier studies have reported higher sorption of As(V) compared to As(III) to AHA and

338   SRHA.[18,22,38] However, in the present study with peat this order is found to be exactly opposite,

339   which can be potentially explained by the electrostatic repulsion between peat and As species.

Considering the pKa values of the three As species, at the studied pH range (4.5 and 7.0) the predominant species for As(III) should be neutral H_3AsO_3, whereas for As(V) and MTAs(V) it should be negatively charged $H_2AsO_4^-/HAsO_4^{2-}$ and $H_2AsSO_3^-/HAsSO_3^{2-}$, respectively.[1,45] Possibly, because of higher acidity of the functional groups, the studied peat is more negatively charged than AHA and SRHA at a specific pH. Therefore, compared to AHA and SRHA, when As(V) and MTAs(V) were equilibrated with peat the effect of electrostatic repulsion between more negatively charged peat and negatively charged As species predominated over the effect of higher partial positive charge on the As center in these two species, resulting in lower sorption. On the other hand, since the predominant As (III) species at the studied pH was neutral, the electrostatic repulsion between negatively charged peat and neutral As species would be low, resulting in higher complexation, despite lower partial positive charge on the As center. This electrostatic repulsion can also explain the more prominent pH effect for As(III) complexation compared to As(V) complexation to peat (Figure 1). During change of pH from 4.5 to 7.0 the effect of increased nucleophilicity of the alcoholic group was largely offset by the increased electrostatic repulsion between the negatively charged peat and As(V) species; whereas, for As(III) this offset was small because of involvement of the neutral species in the complexation. Furthermore, this electrostatic repulsion was also probably responsible for the increased R_{As-C} and CN_{As-C} in As(V)- and MTAs(V)-treated peat compared to that in As(III)-treated peat (Table 1). It is worth recalling that in the study of Hoffmann et al.[26] the R_{As-C} in Fe-spiked peat equilibrated with As(III) was longer at pH ≥8.4 than at pH 7.0, which can also be due to the formation of predominantly negatively charged $H_2AsO_3^-$ species at these pH, which are close to the pKa1 of H_3AsO_3 (9.2),[1] resulting in increased electrostatic repulsion. Despite electrostatic repulsion, the driving force for complexation of the As species to alcoholic group of NOM has been attributed to the stability gained by donation of the negative charge of the alkoxide ion (R-O^-) to the partially positively charged As atom and/or additional chelation and hydrogen bonding with nearby functional group.[18]

Environmental implication. This study shows that alcoholic groups of NOM can be an alternative or additional binding site for the binary complexation of different As species to NOM. Although the extent of binding is considerably less compared to the binary complexation through organic thiol groups, it is comparable to the binding through Fe^{3+} bridged ternary complex formation. This study implis that NOM can still be a potential sorbent for different As

species in systems that are deficient in polyvalent metal cations for ternary complex formation and where organic thiol group content in NOM is not high enough to make significant thiol coordination. Such conditions may prevail in anoxic sulfur deficient ombrotrophic peat bogs, in paddy soils, or aquifer sediments in Bangladesh and West Bengal, India, where the extent of As toxicity to the local inhabitants is most severe. However, similar complexation in the aqueous phase may increase the mobility of As species, but decrease their toxicity by decreasing free ion concentration. This study further implies that the determination of acidity of the functional groups in NOM is essential to assess the mobility of different As species in NOM-rich environments. When the acidity of the functional groups is high, complexation of As(III) is more compared to As(V) and MTAs(V) and vice versa. Therefore, in systems, where NOM is the predominant sorbent for As species, depending on acidity of the functional groups of NOM, As(V) can have a higher mobility than As(III); this is contrasting to the general assumption often made of arsenate being more mobile than arsenite in the environment.[1]

SUPPORTING INFORMATIONS

Additional tables, figures, and analytical methods.

REFERENCES

(1)   Smedley, P. L.; Kinniburgh, D. G. Source and Behaviour of Arsenic in Natural Waters.

Appl. Geochem. **2002**, *17*, 517–568.

(2)   Nordstrom, D. K. Of Arsenic in Ground Water. *Science* **2002**, *296*, 64–65.

(3)   Brammer, H.; Ravenscroft, P. Arsenic in Groundwater: A Threat to Sustainable Agriculture in South and South-East Asia. *Environ. Int.* **2009**, *35* (3), 647–654.

(4)   Fendorf, S.; Michael, H. A.; Van Geen, A. Spatial and Temporal Variations of Groundwater Arsenic in South and Southeast Asia. *Science* **2010**, *328*, 1123–1127.

(5)   Stauder, S.; Raue, B.; Sacher, F. Thioarsenates in Sulfidic Waters. *Environ. Sci. Technol.* **2005**, *39* (16), 5933–5939.

(6)   Planer-Friedrich, B.; London, J.; Mccleskey, R. B.; Nordstrom, D. K.; Wallschläger, D. Thioarsenates in Geothermal Waters of Yellowstone National Park: Determination, Preservation, and Geochemical Importance. *Environ. Sci. Technol.* **2007**, *41* (15), 5245–5251.

(7)   Wallschläger, D.; Stadey, C. J. Determination of (Oxy)Thioarsenates in Sulfidic Waters. *Anal. Chem.* **2007**, *79* (10), 3873–3880.

(8)   Planer-Friedrich, B.; Suess, E.; Scheinost, A. C.; Wallschlager, D. Arsenic Speciation in Sulfidic Waters : Reconciling Contradictory Spectroscopic and Chromatographic Evidence. *Anal. Chem.* **2010**, *82*, 10228–10235.

(9)   Suess, E.; Wallschläger, D.; Planer-Friedrich, B. Stabilization of Thioarsenates in Iron-Rich Waters. *Chemosphere* **2011**, *83* (11), 1524–1531.

(10) Stucker, V. K.; Williams, K. H.; Robbins, M. J.; Ranville, J. F. Arsenic Geochemistry in a Biostimulated Aquifer: An Aqueous Speciation Study. *Environ. Toxicol. Chem.* **2013**, *32* (6), 1216–1223.

(11) Stucker, V. K.; Silverman, D. R.; Williams, K. H.; Sharp, J. O.; Ranville, J. F. Thioarsenic

424   Species Associated with Increased Arsenic Release during Biostimulated Subsurface

425   Sulfate Reduction. *Environ. Sci. Technol.* **2014**, *48* (22), 13367–13375.

426 (12) Dixit, S.; Hering, J. Comparison of Arsenic (V) and Arsenic (III) Sorption onto Iron Oxide

427   Minerals: Implications for Arsenic Mobility. *Environ. Sci. Technol.* **2003**, *37* (18), 4182–

428   4189.

429 (13) Couture, R. M.; Rose, J.; Kumar, N.; Mitchell, K.; Wallschläger, D.; Van Cappellen, P.

430   Sorption of Arsenite, Arsenate, and Thioarsenates to Iron Oxides and Iron Sulfides: A

431   Kinetic and Spectroscopic Investigation. *Environ. Sci. Technol.* **2013**, *47* (11), 5652–5659.

432 (14) Biswas, A.; Gustafsson, J. P.; Neidhardt, H.; Halder, D.; Kundu, A. K.; Chatterjee, D.;

433   Berner, Z.; Bhattacharya, P. Role of Competing Ions in the Mobilization Ofarsenic in

434   Groundwater of Bengal Basin: Insight from Surface Complexation Modeling. *Water Res.*

435   **2014**, *55*, 30–39.

436 (15) Redman, A. D.; Macalady, D.; Ahmann, D. Natural Organic Matter Affects Arsenic

437   Speciation and Sorption onto Hematite. *Environ. Sci. Technol.* **2002**, *36* (13), 2889–2896.

438 (16) Wang, S.; Mulligan, C. N. Effect of Natural Organic Matter on Arsenic Release from

439   Soils and Sediments into Groundwater. *Environ. Geochem. Health* **2006**, *28* (3), 197–214.

440 (17) Ritter, K.; Aiken, G. R.; Ranville, J. F.; Bauer, M.; Macalady, D. L. Evidence for the

441   Aquatic Binding of Arsenate by Natural Organic Matter - Suspended Fe(III). *Environ. Sci.*

442   *Technol.* **2006**, *40* (17), 5380–5387.

443 (18) Buschmann, J.; Kappeler, A.; Lindauer, U.; Kistler, D.; Berg, M.; Sigg, L. Arsenite and

444   Arsenate Binding to Dissolved Humic Acids: Influence of PH, Type of Humic Acid, and

445   Aluminum. *Environ. Sci. Technol.* **2006**, *40* (19), 6015–6020.

446 (19) Bauer, M.; Blodau, C. Arsenic Distribution in the Dissolved, Colloidal and Particulate

447   Size Fraction of Experimental Solutions Rich in Dissolved Organic Matter and Ferric

448   Iron. *Geochim. Cosmochim. Acta* **2009**, *73* (3), 529–542.

449 (20) Sharma, P.; Rolle, M.; Kocar, B. D.; Fendorf, S.; Kapppler, A. Influence of Natural

450   Organic Matter on As Transport and Retention. *Environ. Sci. Technol.* **2011**, *45* (2), 546–

451   553.

452 (21) Langner, P.; Mikutta, C.; Kretzschmar, R. Arsenic Sequestration by Organic Sulphur in

453   Peat. *Nat. Geosci.* **2012**, *5* (1), 66–73.

454 (22) Thanabalasingam, P.; Pickering, W. F. Arsenic Sportion by Humic Acids. *Environ. Pollut.*

455   *Ser. B, Chem. Phys.* **1986**, *12* (3), 233–246.

456 (23) Sharma, P.; Ofner, J.; Kappler, A. Formation of Binary and Ternary Colloids and

457   Dissolved Complexes of Organic Matter, Fe and As. *Environ. Sci. Technol.* **2010**, *44*,

458   4479–4485.

459 (24) Mikutta, C.; Kretzschmar, R. Spectroscopic Evidence for Ternary Complex Formation

460   between Arsenate and Ferric Iron Complexes of Humic Substances. *Environ. Sci. Technol.*

461   **2011**, *45*, 9550–9557.

462 (25) Liu, G.; Fernandez, A.; Cai, Y. Complexation of Arsenite with Humic Acid in the

463   Presence of Ferric Iron. *Environ. Sci. Technol.* **2011**, *45*, 3210–3216.

464 (26) Hoffmann, M.; Mikutta, C.; Kretzschmar, R. Arsenite Binding to Natural Organic Matter:

465   Spectroscopic Evidence for Ligand Exchange and Ternary Complex Formation. *Environ.*

466   *Sci. Technol.* **2013**, *47* (21), 12165–12173.

467 (27) Hoffmann, M.; Mikutta, C.; Kretzschmar, R. Bisulfide Reaction with Natural Organic

468   Matter Enhances Arsenite Sorption: Insights from X - Ray Absorption Spectroscopy.

469   *Environ. Sci. Technol.* **2012**, *46*, 11788–11797.

470 (28) Hoffmann, M.; Mikutta, C.; Kretzschmar, R. Arsenite Binding to Sulfhydryl Groups in the
471   Absence and Presence of Ferrihydrite : A Model Study. *Environ. Sci. Technol.* **2014**, *48*,
472   3822–3831.

473 (29) Catrouillet, C.; Davranche, M.; Dia, A.; Bouhnik-Le Coz, M.; Pédrot, M.; Marsac, R.;
474   Gruau, G. Thiol Groups Controls on Arsenite Binding by Organic Matter: New
475   Experimental and Modeling Evidence. *J. Colloid Interface Sci.* **2015**, *460*, 310–320.

476 (30) Catrouillet, C.; Davranche, M.; Dia, A.; Bouhnik-Le Coz, M.; Demangeat, E.; Gruau, G.
477   Does As(III) Interact with Fe(II), Fe(III) and Organic Matter through Ternary Complexes?
478   *J. Colloid Interface Sci.* **2016**, *470*, 153–161.

479 (31) Liu, G.; Cai, Y. Complexation of Arsenite with Dissolved Organic Matter: Conditional
480   Distribution Coefficients and Apparent Stability Constants. *Chemosphere* **2010**, *81* (7),
481   890–896.

482 (32) Tipping, E.; Hurley, M. . A Unifying Model of Cation Binding by Humic Substances.
483   *Geochim. Cosmochim. Acta* **1992**, *56* (10), 3627–3641.

484 (33) Lenoble, V.; Dang, D. H.; Loustau Cazalet, M.; Mounier, S.; Pfeifer, H. R.; Garnier, C.
485   Evaluation and Modelling of Dissolved Organic Matter Reactivity toward As^{III} and As^{V} -
486   Implication in Environmental Arsenic Speciation. *Talanta* **2015**, *134*, 530–537.

487 (34) Guenet, H.; Davranche, M.; Vantelon, D.; Bouhnik-Le Coz, M.; Jarde, E.; Dorcet, V.;
488   Demangeat, E.; Jestin, J. Highlighting the Wide Variability in Arsenic Speciation in
489   Wetlands: A New Insight into the Control of the Behavior of Arsenic. *Geochim.*
490   *Cosmochim. Acta* **2017**, *203*, 284–302.

491 (35) Besold, J.; Biswas, A.; Suess, E.; Scheinost, A. C.; Rossberg, A.; Mikutta, C.;
492   Kretzschmar, R.; Gustafsson, J. P.; Planer-Friedrich, B. Monothioarsenate Transformation

493   Kinetics Determining Arsenic Sequestration by Sulfhydryl Groups of Peat. *Environ. Sci.*

494   *Technol.* **2018**, *52*, 7317–7326.

495 (36) Suess, E.; Scheinost, A. C.; Bostick, B. C.; Merkel, B. J.; Wallschlaeger, D.; Planer-

496   Friedrich, B. Discrimination of Thioarsenites and Thioarsenates by X-Ray Absorption

497   Spectroscopy. *Anal. Chem.* **2009**, *81* (20), 8318–8326.

498 (37) Härtig, C.; Planer-Friedrich, B. Thioarsenate Transformation by Filamentous Microbial

499   Mats Thriving in an Alkaline, Sulfidic Hot Spring. *Environ. Sci. Technol.* **2012**, *46* (8),

500   4348–4356.

501 (38) Warwick, P.; Inam, E.; Evans, N. Arsenics Interaction with Humic Acid. *Environ. Chem.*

502   **2005**, *2* (2), 119–124.

503 (39) Kamenar, B.; Bruvo, M.; Butumović, J. Structures Involving Unshared Electron Pair. The

504   Crystal Structures of As(OCOCH3)3 and As2O(OCOCH3)4. *Zeitschrift für Anorg. und*

505   *Allg. Chemie* **1993**, *619* (5), 943–946.

506 (40) Ona-Nguema, G.; Morin, G.; Juillot, F.; Calas, G.; Brown, G. E. EXAFS Analysis of

507   Arsenite Adsorption onto Two-Line Ferrihydrite, Hematite, Goethite, and Lepidocrocite.

508   *Environ. Sci. Technol.* **2005**, *39* (23), 9147–9155.

509 (41) Kitahama, K.; Kiriyama, R.; Baba, Y. Refinement of the Crystal Structure of Scorodite.

510   *Acta Crystallogr. Sect. B* **1975**, *31* (1), 322–324.

511 (42) Lang, W. R.; Mackey, J. F.; Gortner, R. A. Some Esters of Arsenious Acid. *J. Chem. Soc.,*

512   *Trans.* **1908**, *93*, 1364–1372.

513 (43) Brill, T. B.; Campbell, N. C. Arsenites and Antimonites. 11. Vibrational, Nuclear

514   Quadrupole Resonance, and Mass Spectral Properties of Arsenic(II1) and Antimony(II1)

515   Esters and Thioesters'. *Inorg. Chem.* **1973**, *12* (8), 1884–1888.

516   (44)   Tsivgoulis, G. M.; Ioannou, P. V. Esterification Equilibrium Constants of Arsonic and

517   Arsinic Acids. *Monatshefte fur Chemie* **2012**, *143* (12), 1603–1608.

518   (45)   Thilo, E.; Hertzog, K.; Winkler, A. Über Vorgänge Bei Der Bildung Des Arsen(V)-Sulfids

519   Beim Ansäuern von Tetrathioarsenatlösungen. *Zeitschrift für Anorg. und Allg. Chemie*

520   **1970**, *373*, 111–121.

521

522

TABLE CAPTIONS

Table 1: EXAFS parameters determined by shell-fit analysis of the As K edge EXAFS spectra

of the peat equilibrated with different concentrations of As(III) and As(V) at pH 4.5 and 7.0 and

MTAs(V) at pH 7.0 only.

Table 1: EXAFS parameters determined by shell-fit analysis of the As K edge EXAFS spectra of the peat equilibrated with different concentrations of As(III) and As(V) at pH 4.5 and 7.0 and MTAs(V) at pH 7.0 only.

As species	Sample label	k-range	As-O			As-S			As-C			$\Delta E_0{}^a$	R-factor[b]	redχ^{2c}
			CN^d	R^e (Å)	σ^{2f} (Å^2)	CN	R (Å)	σ^2 (Å^2)	CN	R (Å)	σ^2 (Å^2)	(eV)	(%)	
As(III)	7.0/1000	2.2-13.0	**3.0**[g]	1.80(0[h])	0.0022(3)				1.7(4)	2.74(3)	**0.0059**[i]	0.9(6)	1.5	362
	7.0/150	2.2-9.5	**3.0**	1.78(0)	0.0023(3)				1.0(3)	2.73(4)	**0.0059**	1.6(7)	0.6	60
	7.0/100	2.2-11.0	**3.0**	1.79(0)	0.0031(3)				1.4(3)	2.73(3)	**0.0059**	1.4(6)	1.0	62
	4.5/1000	2.2-12.0	**3.0**	1.80(0)	0.0010(4)				2.1(5)	2.73(3)	**0.0059**	1.1(7)	1.7	144
	4.5/500	2.2-12.0	**3.0**	1.80(1)	0.0006(4)				2.4(5)	2.74(3)	**0.0059**	1.4(8)	2.2	122
As(V)	7.0/1000	2.2-12.5	**4.0**	1.69(0)	0.0016(4)				3.2(10)	2.84(2)	**0.0059**	1.7(8)	1.7	407
	7.0/500	2.2-12.5	**4.0**	1.69(1)	0.0009(5)				3.4(14)	2.82(3)	**0.0059**	1.3(11)	3.4	372
	7.0/250	2.2-12.0	**4.0**	1.68(1)	0.0011(4)				3.1(11)	2.82(3)	**0.0059**	2.1(9)	2.3	110
	4.5/1000	2.2-12.5	**4.0**	1.69(1)	0.0017(4)				3.0(10)	2.82(4)	**0.0059**	0.9(9)	2.1	315
	4.5/500	2.2-12.0	**4.0**	1.68(1)	0.0006(5)							-0.8(9)	3.2	260
MTAs(V)	7.0/1000	2.2-12.5	**3.0**	1.71(0)	0.0034(4)	**1.0**	2.08(1)	0.0042(9)	2.6(5)	2.78(2)	**0.0059**	1.0(6)	0.7	171
	7.0/150	2.2-10.5	**3.0**	1.72(1)	0.0045(5)	**1.0**	2.10(1)	0.0048(10)	2.9(5)	2.82(2)	**0.0059**	1.6(7)	0.6	60
	7.0/100	2.2-10.0	**3.0**	1.72(1)	0.0031(5)	**1.0**	2.11(1)	0.0027(11)	3.4(7)	2.81(2)	**0.0059**	1.0(9)	0.8	33

[a]Energy-shift parameter, was the same for all paths. [b]R-factor = Σ_i(data$_i$ – fit$_i$)^2/$\Sigma_i$data). [c]redχ^2 = (N$_{idp}$/N$_{pts}$)Σ_i((data$_i$ – fit$_i$)/ε_i)^2 (N$_{idp}$ – N$_{var}$)$^{-1}$, where N$_{idp}$: the number of independent points in the model fit, N$_{pts}$: the total number of data points, N$_{var}$: the number of variables in the fit, ε_i: the uncertainty in the ith data point. [d]Coordination number (path degeneracy). [e]Interatomic distance or mean half path length (bond distance for atom in the first-shell). [f]Debye – Waller parameter. [g]Values in bold were fixed in the fit. [h]Values in parenthesis represent uncertainty in the last significant figure of the fitted parameters. [i]This value was determined by fitting the TEA (reference standard) spectrum. Various multiple scattering paths (see text for details) were included in the fit and constrained in terms of three single scattering paths (Table SI-1). Passive amplitude reduction factor (S$_0{}^2$) was set to 1.0 for shell-fit analysis of all the samples.
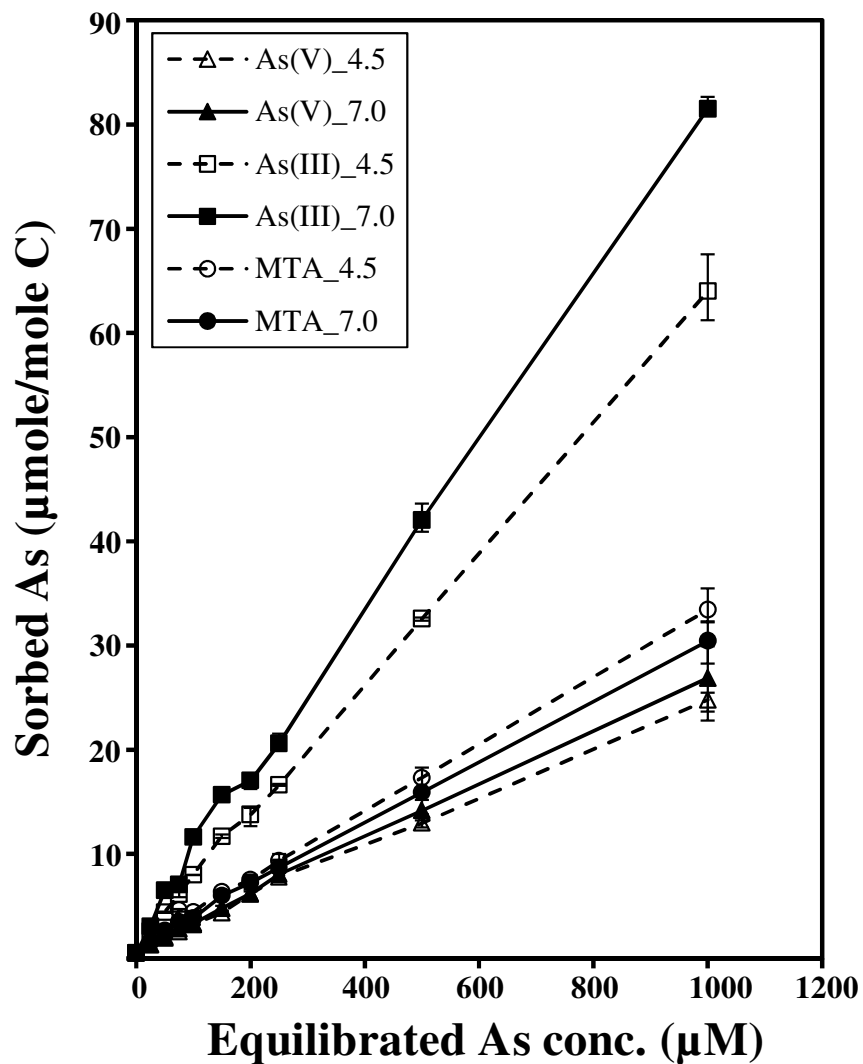
FIGURE CAPTIONS

541 Figure 1: Sorption of three As species to peat at different equilibrated concentrations at pH 4.5
542 and 7.0. Symbol and replicate represent average and range of the three replicates.

543 Figure 2: k^3-Weighted As K edge EXAFS spectra and magnitude and real part of the Fourier
544 transforms (FT) of (A) As(III), (B) As(V), and (C) MTAs(V). Grey lines and red dots represent
545 data and model fit, respectively. Sample labels represent equilibrated pH and As concentration.
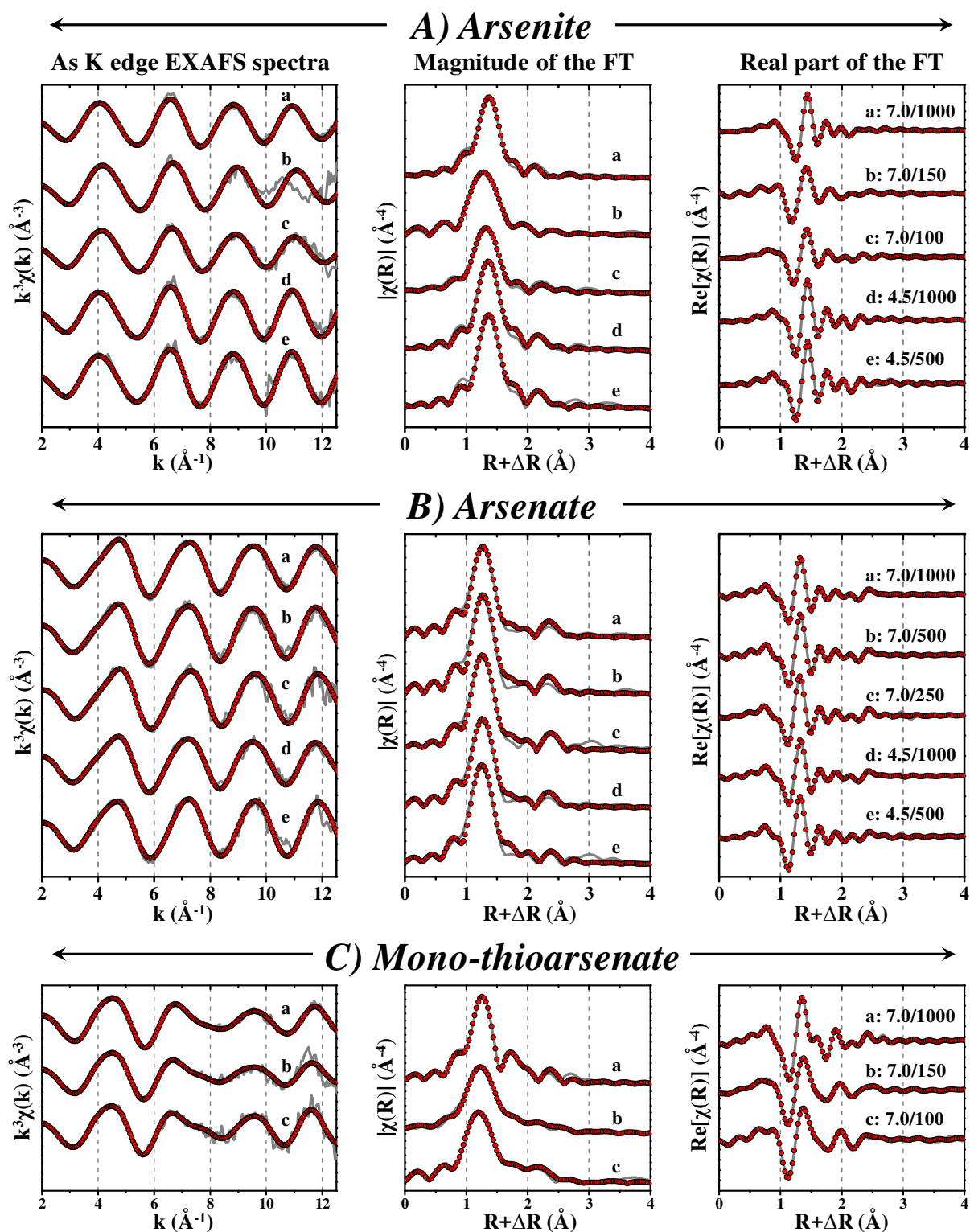
546 Figure 3: Schematic presentation of complexes of the three As species with alcoholic group (for
547 simplicity shown as phenol) of peat identified in the present study: (A) monodentate binding of
548 As(III) at ≤0.69 mmol As(III)/mol C, (B) bidentate binding As(III) at ≥2.3 mmol As(III)/mol,
549 (C) tridentate binding of As(V), and (D) tridentate binding of MTAs(V). Color code of the
550 sphere: purple – As, blue – O, yellow – S, and black – C.
551
552

553

554   **Figure 1:** Sorption of three As species to peat at different equilibrated concentrations at pH 4.5

555   and 7.0. Symbol and replicate represent average and range of the three replicates.

556

557

Figure 2: k^3-Weighted As K edge EXAFS spectra and magnitude and real part of the Fourier transforms (FT) of (A) As(III), (B) As(V), and (C) MTAs(V). Grey lines and red dots represent data and model fit, respectively. Sample labels represent equilibrated pH and As concentration.
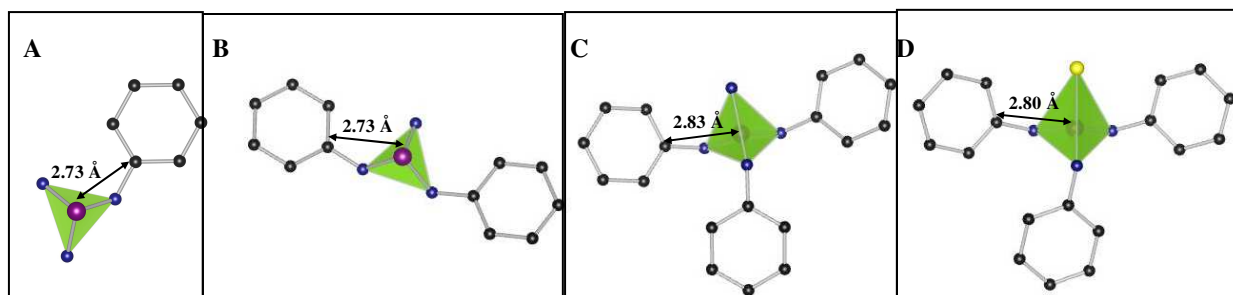
Figure 3: Schematic presentation of complexes of the three As species with alcoholic group (for simplicity shown as phenol) of peat identified in the present study: (A) monodentate binding of As(III) at ≤0.69 mmol As(III)/mol C, (B) bidentate binding As(III) at ≥2.3 mmol As(III)/mol, (C) tridentate binding of As(V), and (D) tridentate binding of MTAs(V). Color code of the spheres: purple – As, blue – O, yellow – S, and black – C.